Magnetic circular dichroism at transition metal $L_{2,3}$ edges in $D0_3$-type $(Fe_{1-x}Mn_x)_3Al$ alloys

Kazuo Soda,[a]* Osamu Yoshimoto,[a] Hiroshi Nozaki,[a] Tsunehiro Takeuchi,[a] Uichiro Mizutani,[a] Hideaki Kato,[b] Masaaki Kato,[b] Yoichi Nishino,[b] Shin Imada,[c] Shigemasa Suga,[c] Tomohiro Matsushita[d] and Yuji Saitoh[e]

[a]Graduate School of Engineering, Nagoya University, Furo-cho, Chikusa-ku, Nagoya 464-8603 Japan, [b]Department of Materials Science and Engineering, Nagoya Institute of Technology, Gokiso-cho, Showa-ku, Nagoya 466-8555 Japan, [c]Graduate School of Engineering Science, Osaka University, Machikaneyama, Toyonaka 560-8531 Japan, [d]Japan Synchrotron Radiation Research Institute, Kouto, Mikazuki-cho, Sayo-gun, Hyogo 679-5198 Japan, and [e]Department of Synchrotron Radiation Research, Japan Atomic Energy Research Institute, Kouto, Mikazuki-cho, Sayo-gun, Hyogo 679-5148 Japan.
E-mail: j45880a@nucc.cc.nagoya-u.ac.jp

We have measured magnetic circular dichroism (MCD) spectra at the transition-metal $L_{2,3}$ edges in $D0_3$-type $(Fe_{1-x}Mn_x)_3Al$ in order to investigate their local magnetic moments. The analysis of the spectra shows that Fe has moments much larger than Mn, whose moment is ferromagnetically coupled with the Fe one. This does not lend support to the antiferromagnetic mechanism proposed for the reduction in magnetization as well as a large Mn moment predicted for x = 1/3. The evolution of satellites found in the Mn spectrum with x increased suggests that the change in the electronic state may result in the magnetization reduction.

Keywords: magnetic circular dichroism, local magnetic moments, $D0_3$-type $(Fe_{1-x}Mn_x)_3Al$ alloys, Fe $L_{2,3}$ edges, Mn $L_{2,3}$ edges.

1. Introduction

The $D0_3$-type pseudo-binary $(Fe_{1-x}T_x)_3Al$ alloys, where T is a 3d transition metal element to the left side of Fe in the periodic table, exhibit an anomalous negative temperature dependence of their electrical resistivity as well as remarkable reduction in the magnetization and Curie temperature upon the partial substitution of T for Fe (Nishino *et al*., 1997). In these alloys, T preferentially occupies one of the two nonequivalent Fe sites (the Fe(I) site), *i.e.* a site of Fe surrounded with eight Fe atoms as first nearest neighbors. The reduction in magnetization for $(Fe_{1-x}Mn_x)_3Al$ has been attributed to the parasitic antiferromagnetism or Fe-Mn antiferromagnetic coupling (Mager *et al*., 1979). On the other hand, a recent theoretical study has predicted a ferromagnetic coupling between Fe and Mn for the $L2_1$-type Fe_2MnAl, *i.e.* for x = 1/3 in $(Fe_{1-x}T_x)_3Al$ (Fujii *et al*., 1995).

In this study, we have measured magnetic circular dichroism (MCD) spectra at the transition-metal $L_{2,3}$ edges in the $D0_3$-type $(Fe_{1-x}Mn_x)_3Al$ in order to investigate their local magnetic moments. The magneto-optical sum rules for the core-level absorption (Carra *et al*., 1993, Stöhr & König, 1995, Thole *et al*., 1992) allow us to determine the spin and orbital contributions, μ_{spin} and μ_{orbit}, to the magnetic moment separately for a given element at a specific site. The MCD spectrum also exhibits finer structures than the normal X-ray absorption (XAS) spectrum, and, hence, will bring further information on the electronic states involved.

2. Experimental

MCD measurements were performed at the beamline BL25SU of SPring-8, an 8 GeV electron storage ring of the Japan Synchrotron Radiation Research Institute. In this beamline, circularly polarized soft X-ray from a twin helical undulator was monochromatized with a spherical grating monochromator and focused on the sample position through pinholes of a permanent magnet circuit (Saitoh *et al*., 1998). Total photoelectric yields α_P and α_A were measured at 20K in the applied magnetic field of B = 1.4 T along the direction parallel and anti-parallel, respectively, to the soft X-ray photon spin. In the present study, the XAS is defined as an average of these yields, $(\alpha_P+\alpha_A)/2$, and the MCD as a difference, $\alpha_P-\alpha_A$. Photon energy was calibrated by photoelectron measurement of the Au $4f_{5/2}$ core level with its binding energy of 84.0 eV and the detector work function of 4.3 eV. The $D0_3$-type $(Fe_{1-x}Mn_x)_3Al$ alloys were prepared in a size of 5 x 5 x 1 mm^3 for the MCD measurement. Details of the sample preparation are described elsewhere (Nishino *et al*., 1997). Clean surfaces were obtained for the photoelectric yield measurements by *in situ* scraping specimens with a diamond file under a pressure of 3-5 x 10^{-8} Pa.

3. Results and Discussion

Typical MCD spectra are shown in Fig.1 (a) and (b) for the Fe and Mn $L_{2,3}$ edges of the $D0_3$-type $(Fe_{1-x}Mn_x)_3Al$ (x = 0, 0.1, 0.2, and 1/3), respectively, together with the $L_{2,3}$ XAS spectra of Fe_2MnAl. In the figure, these XAS and MCD spectra are normalized so that the spectral intensity at each L_3 edge is unity in the XAS spectrum. Large MCD signals are observed for the Fe $L_{2,3}$ edges, whereas the Mn $L_{2,3}$ MCD spectrum has a relatively small intensity with some satellites, indicated by arrows, in the low energy side of the main lines. As the Mn composition x increases, the Fe $L_{2,3}$ MCD spectra normalized with respect to the Fe composition remain almost unchanged in shape below x = 0.2, while the Mn ones show the reduction in its intensity and the evolution of the satellites. Furthermore, the present results decisively reveal a ferromagnetic coupling between the magnetic moments on Mn and Fe, because the signs of MCD at the L_2 and L_3 edges of Mn are the same as those of Fe, respectively.

Figure 2 shows μ_{spin} and μ_{orbit} estimated on the basis of the magneto-optical sum rules (Carra *et al*., 1993, Stöhr & König, 1995, Thole *et al*., 1992) under the assumption that a number of the 3d holes n_H is 4 for Fe and 5 for Mn irrespective of x. Here, we ignored the contribution of the magnetic dipole, which may be averaged to zero for the polycrystalline sample, and subtracted the backgrounds arising from the transitions to the continuous states by using two appropriate step-like functions in order to evaluate the integrated XAS intensities. Total magnetic moments $\mu_{total} = \mu_{spin} + \mu_{orbit}$ are also shown in Fig.2. As is seen in the figure, the orbital moments on both Fe and Mn are almost quenched, but their spin parts are obviously responsible for their magnetization.

The total moment of 2.2 μ_B for Fe in Fe_3Al is slightly larger than that of 1.8 μ_B estimated from the magnetization (Kato *et al*., 2000). This may be due partly to the assumed large n_H. Indeed, band calculations predicted n_H = 3.8 on average for Fe_3Al (Ishida *et al*., 1976). On the other hand, Teramura *et al*. (1996) pointed out that the spin sum rule underestimates μ_{spin} due to the Coulomb interaction and that its correction may amount to more than 30% for

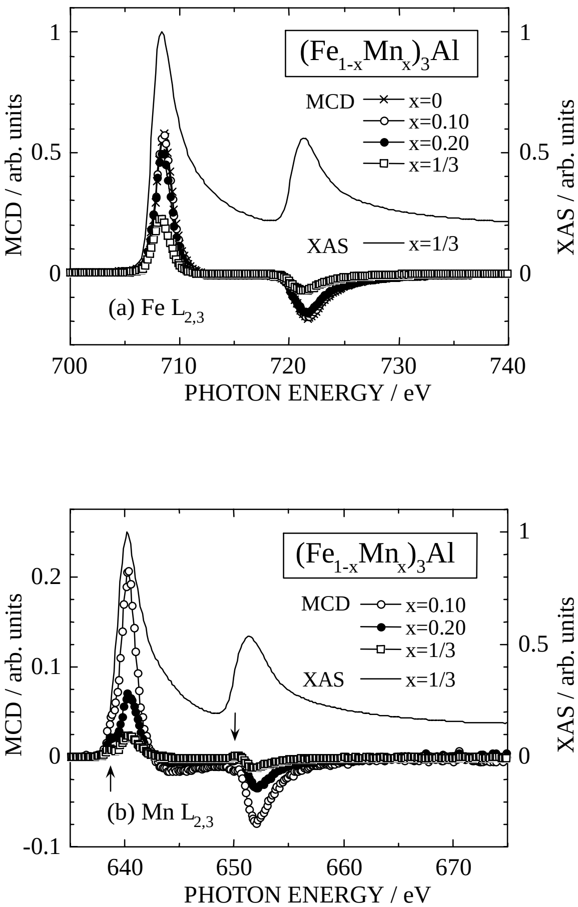

Figure 1
Magnetic circular dichroism spectra (MCD) at the $L_{2,3}$ edges of Fe (a) and Mn (b) in the $D0_3$-type $(Fe_{1-x}Mn_x)_3Al$ with the various Mn composition x. X-ray absorption spectra (XAS) at these $L_{2,3}$ edges are also shown for x=1/3 *i.e.* Fe_2MnAl. Arrows indicate satellite structures.

Mn^{2+} and 10% for Fe^{2+}. Thus, Mn moments are expected to have somewhat larger values than those shown in Fig.2. However, the results presented in Fig.2 clearly show the possession of the Mn moment smaller than the Fe one and the existence of the Mn-Fe ferromagnetic coupling.

The present results agree well with the prediction for the Mn-Fe ferromagnetic coupling in Fe_2MnAl except for the size of the moments; the calculated Mn and Fe moments are 2.35 and 0.16μ_B, respectively (Fujii *et al*., 1995). Relatively large reduction in the Mn moment with increasing x might suggest the antiferromagnetic interaction between the Mn moments in the Fe(I) sublattice or those in the two nonequivalent Fe sublattices arising from the antisite disordering. The observed ferromagnetic coupling is supported by the measured magnetization curve of Fe_2MnAl showing a ferromagnetic hysteresis loop and the absence of antiferromagnetic spin flip up to 5 T, and is apparently inconsistent with the parasitic antiferromagnetism proposed for the magnetization reduction (Mager *et al*., 1979). Furthermore, the evolution of the satellites in the Mn MCD spectrum indicates a change in the electronic states with the Mn substitution through the hybridization between Mn and Fe d states. We consider that the MCD satellites might be related to the low-energy XAS features found in a theoretical study on the $L_{2,3}$ XAS spectrum (de Groot *et al*., 1990). These features evolve as the crystal field is increased, which could lower μ_{spin} on Mn. In metallic compounds, the XAS fine structures are often smeared out due to the screening effect, but fine structures may become prominent in the MCD spectrum. Further theoretical study on the MCD fine structures will clarify the electronic structure and related magnetic properties of $(Fe_{1-x}Mn_x)_3Al$.

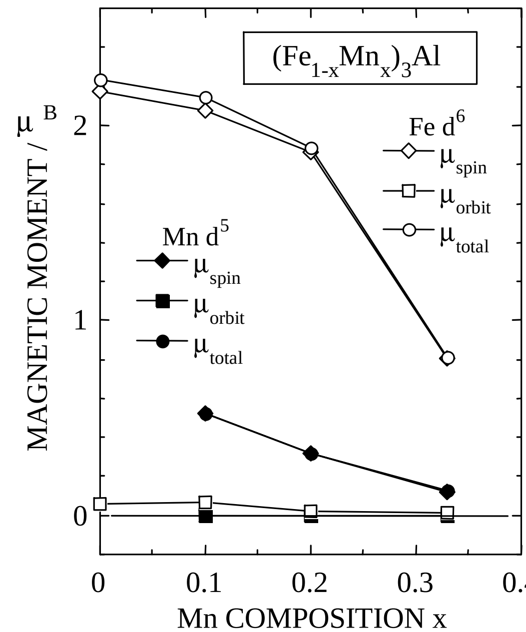

Figure 2
Spin (diamonds) and orbital (squares) parts of the total magnetic moments (circles) on Fe (open symbols) and Mn (closed symbols) of the $D0_3$-type $(Fe_{1-x}Mn_x)_3Al$ with the various Mn composition x.

The synchrotron radiation experiments were performed at the SPring-8 with the approval of the Japanese Synchrotron Radiation Research Institute (JASRI) (Proposal No. 1999A0302-NS-np). We would like to appreciate the staff members of the SPring-8, especially Dr. T. Muro, Dr. M. Kotsugi, and Dr. R. Jung for their support during the course of the MCD measurement.

References

Carra, P., Thole, B.T., Altarelli, M. & Wang, X. (1993) *Phys. Rev. Lett.* **70**, 694-697.
de Groot, F.M.F., Fuggle, J.C., Thole, B.T. & Sawatzky, G.A. (1990) *Phys. Rev. B* **42**, 5459-5468.
Fujii, S., Ishida, S. & Asano, S. (1995) *J. Phys. Soc. Jpn.* **64**, 185-191.
Ishida, S., Ishida, J., Asano, S. & Yamashita, J. (1976) *J. Phys. Soc. Jpn.* **41**, 1570-1574.
Kato, M., Nishino, Y., Mizutani, U. & Asano, S. (2000) *J. Phys.: Codens. Matter* **12**, 1769-1779.
Major S., Wieser, E., Zemcík, T., Schneeweiss, O., Stetsenko, P.N. & Surikov, V.V. (1979) *Phys. Stat. Sol.* (a) **52**, 249-258.
Nishino, Y., Kumada, C. & Asano, S. (1997) *Scripta Mater.* **36**, 461-466.
Saito, Y., Nakatani, T., Matsushita, T., Miyahara, T., Fujisawa, M., Soda, K., Muro, T., Ueda, S., Harada, H., Sekiyama, A., Imada, S., Daimon, H. & Suga, S. (1998) *J. Synchrotron Rad.* **5**, 542-544.
Stöhr, J. & König, H. (1995) *Phys. Rev. Lett*. **75**, 3748-3751.
Teramura, Y., Tanaka, A. & Jo, T. (1996) *J. Phys. Soc. Jpn*. **65**, 1053-1055.
Thole, B.T., Carra, P., Sette, F., & van der Laan, G. (1992) *Phys. Rev. Lett.* **68**, 1943-1946.